Caiani *et al. Bioelectronic Medicine* (2026) 12:1
https://doi.org/10.1186/s42234-025-00198-1

Bioelectronic Medicine

RESEARCH Open Access

Resonant core–shell magnetoelectric nanoparticles as sensors of neural magnetic activity: a computational study

Giulia Caiani[1,2*], Emma Chiaramello[2], Paolo Ravazzani[2] and Serena Fiocchi[2]

Abstract

Measuring the weak magnetic fields generated by spontaneous biological activity, such as those produced in the brain or heart, offers complementary information to conventional electrophysiological techniques, as electroencephalography and electrocardiography. Nevertheless, the widespread clinical use of biomagnetic sensing is hindered by the bulky and costly technology currently available, including SQUID-based and optically pumped magnetometers. In recent years magnetoelectric materials have been explored as highly sensitive, room-temperature magnetic field sensors, offering a compelling alternative to conventional approaches. Here, we investigate the feasibility of using resonant magnetoelectric nanoparticles (MENPs) as nanoscale magnetic sensors by exploiting the delta-E effect, in which magnetic-field–induced changes in elastic properties, i.e. Young's modulus, shift the nanoparticle's resonance frequency. Using a computational modeling approach, we first developed and characterized a core–shell MENP model. We then identified its natural resonance frequencies in the GHz range, evaluated its sensitivity to external magnetic field variations, and determined the optimal bias static magnetic field and core radius for maximum sensitivity. Finally, we assessed the performance of the optimized nanoparticle in detecting neural-level magnetic fields. Our simulations demonstrate that MENP can achieve a maximum sensitivity of 2.59 Hz/nT for a core diameter of 50 nm under a bias static magnetic field of 1000 Oe. These findings highlight both the feasibility of exploiting the delta-E effect in MENPs and the tunability of their structural parameters, which could be tailored for specific applications. In conclusion, this work set the theoretical groundwork for the development of cutting-edge, wireless and non-invasive nanoscale magnetic sensors for neural interfacing and biomedical signals sensing.

Keywords Magnetoelectric nanoparticles, Delta-E effect, Neural activity recordings, Wireless sensing, Computational modelling

*Correspondence:
Giulia Caiani
giulia.caiani@polimi.it
[1]Dipartimento Di Elettronica, Informazione E Bioingegneria (DEIB), Politecnico Di Milano, Milan, Italy
[2]Istituto di Elettronica e di Ingegneria dell'Informazione e delle Telecomunicazioni (IEIIT), Consiglio Nazionale delle Ricerche (CNR), Milan, Italy

Background

The first measurements of the magnetic field generated by the electrical activity of the heart and the brain date back to Cohen's pioneering study in 1972 (Cohen 1972). During the last six decades, the field of biomagnetism has witnessed significant technological advancements, enabling the detection of extremely weak magnetic fields produced by the body (Roth 2023). These magnetic fields span a frequency range from DC to below 1 kHz (Cohen et al. 1970; Sternickel and Braginski 2006; Hayes et al. 2019), with amplitudes reaching up to about 1 nT at 100 μm and few nT inside the neuronal ensemble (Parker and Wikswo 1997; Caruso et al. 2017).

Although electrical activity can be directly recorded, measuring the associated magnetic fields offers distinct and valuable advantages. Unlike electric fields, the magnetic field travels through tissues without distortion, since their relative permittivity is close to that of free space (Pethig 1987). Consequently, magnetic recordings can achieve higher spatial resolution than bioelectric signals, reaching millimetric range for cortical brain areas (Barnes et al. 2004), and allow for more straightforward source-reconstruction. Moreover, electrical recordings such as electroencephalography (EEG) require preparation time to ensure a stable and reliable acquisition, since conductive gel are usually applied to reduce skin–electrode impedance, and recordings are typically not wireless (Soufineyestani et al. 2020). Magnetoencephalography (MEG), in combination with source analysis, yields spatiotemporal maps of brain activation with excellent temporal and good spatial resolution. This is essential for applications such as pre-operative evaluation in brain surgery (e.g. precise localization of epileptic loci (Fred et al. 2022)), studying the dynamics of large-scale neural activation and connectivity in cognitive neuroscience (Gross 2019), and identifying potential electrophysiological markers for early detection of Alzheimer disease (Nakamura et al. 2018). In addition, biomagnetic signals can provide three-dimensional vector information of the neural activity (Dong et al. 2022).

Similarly, magnetocardiography (MCG) is also gaining importance in the clinical management of cardiovascular diseases, particularly for the triage of acute chest pain, diagnosis and prognosis prediction in both chronic and acute coronary syndromes (Li et al. 2025). Several studies have concluded that MCG is more sensitive to triage of acute chest pain and diagnosis of ischemic heart disease than widely used screening tools such as ECG, echocardiography, and stress tests (Park et al. 2005; Tolstrup et al. 2006; Kwon et al. 2010). Moreover, Lombardi and colleagues (Lombardi et al. 2018) found an accuracy of 94.7% of MCG in differentiating benign and malignant ventricular arrhythmia, compared with invasive electrophysiological mapping.

Despite the growing clinical interest in biomagnetism, the introduction of MEG and MCG into routine medical practice remains underexplored due to the technological constraints in signal detection. Specifically, both MEG and MCG still rely on superconducting quantum interference devices (SQUIDs), with achieve femto-Tesla sensitivity, but require bulky, expensive instrumentation, operating in a magnetically shielded and temperature-controlled environment (Körber et al. 2016). Recent innovations, however, suggest potential alternatives: Murzin and colleagues reviewed several emerging non-cryogenic systems to detect biomagnetic field, such as fluxgate, magnetoelectric, giant magneto-impedance, optically pumped, and Hall effect sensors (Murzin et al. 2020).

Among these, magnetoelectric (ME) materials have attracted increasing attention in recent years. ME materials offer several advantages over conventional technologies: they operate at room temperature, require low power, and can achieve detection limits (LOD) in the picoTesla/√Hz range, particularly at low frequencies (DC–1 kHz) (Elzenheimer et al. 2023; Patil et al. 2021; Martins et al. 2024).

These composites directly convert magnetic fields into electrical signals through the coupling between a magnetostrictive and a piezoelectric phase (Eerenstein et al. 2006). Many studies focused on the possibility of using ME materials and nanomaterials, engineered in various geometries, as sources of electric fields in low frequency bands, thus able to interact with tissues in different applications (Dong et al. 2022).

More recently, magnetoelectric nanoparticles (MENPs) have gained attention in the biomedical field, with proposed applications ranging from brain stimulation through direct ME effect (Kujawska and Kaushik 2023; Vezzoni et al. 2025), electric field sensing through the converse ME effect (Galletta et al. 2025; Zhang et al. 2023), targeted drug delivery (Abdelazim 2017), and beyond (Song et al. 2022). Their biocompatibility and feasibility in biological application has been demonstrated by in vivo animal studies (Kozielski, et al. 2021). Core–shell multiferroic nanoparticles exploit strain-mediated interfacial coupling between ferromagnetic and ferroelectric components, with the magnetostrictive core undergoing Joule magnetostriction in presence of an external magnetic field (Ekreem et al. 2007; Srinivasan et al. 2001) and the piezoelectric shell that acts as a strain to electric field converter. The most common composite used in these early applications of MENPs is made of a combination of cobalt ferrite (CFO) and barium titanate (BTO), owing to its good biocompatibility and high magnetoelectric coupling coefficient at room temperature (Hadjikhani et al. 2017; Corral-Flores et al. 2010).

Despite their potential, very few studies have explored the behaviour of these MENPs at their mechanical resonance, where the ME coupling is maximized as a result of enhanced strain transfer between the two phases (Zuo et al. 2020). The on-resonance condition offers the opportunity to use ME structures as probes of low-frequency magnetic field.

Many biomedical applications require high sensitivity in the low-frequency range (DC–1 kHz), where conventional ME sensor performance tends to deteriorate. To address this limitation, a key mechanism known as the delta-E effect has been proposed (Gojdka et al. 2011; Liang et al. 2021). The delta-E effect, defined as the change in the Young's modulus (E) of a magnetostrictive material due to magnetic domain reorientation during magnetization, provides a pathway to enhance sensitivity in this regime. This change in E can be quantified by observing shifts in the mechanical resonance frequency of the sensor, as described by Staruch et al. (2017). So far only very few studies used the ME sensor based on delta-E effect for biomedical applications (Zaeimbashi, et al. 2018; Zuo et al. 2020), and most of these have focused on millimetre-scale structures such as resonators, cantilevers and delay lines, as reported in Dong and colleagues' review (Dong et al. 2022). The use of thin-film ME sensors to detect the weak magnetic fields generated by the heart was first demonstrated by Reermann in 2018 (Reermann et al. 2018).

Investigating MENPs could offer the added advantage of being minimally invasive, in vivo studies have demonstrated the possibility to intravenously inject them without the need of surgery (Nguyen et al. 2021), and potentially suitable for wireless sensing, providing an opportunity to detect magnetic fields deep within the brain without the need for implanted electronics. Moreover, MENPs would not need cryogenic systems since they show magnetoelectric effect at room temperature (Kozielski, et al. 2021).

This work presents a proof-of-concept study investigating the potential use of magnetoelectric nanoparticles to sense magnetic fields arising from spontaneous biological activity. This application has not yet been investigated and therefore represents a novel direction within the broader range of potential ME nanoparticle functionalities. This is achieved through a computational approach, with a particular focus on exploiting the delta-E effect at the nanoscale. Our findings aim to lay the groundwork for future development of miniature ME sensors for non-invasive neural monitoring.

Methods

The possibility to use MENPs as sensors of neural magnetic field, exploiting delta-E effect, was demonstrated through a computational approach. Firstly, a model of a nanoparticle was set and characterized to align with literature experimental behaviours; subsequently, the natural resonance frequencies of the modelled nanoparticle were found; thirdly, the nanoparticle's sensitivity in detecting external magnetic field changes was evaluated and the external static magnetic field (H_{DC}) and core radius that yield to the maximum sensitivity were determined; finally, the sensing performance of the optimized nanoparticle in response to a neural magnetic field was assessed. The steps are detailed explained in the following paragraphs and schematically reported in Fig. 1.

	COMSOL analysis	H excitation	Core diameter	Result
A. ME *Nanoparticle modeling and characterization*	Time dependent analysis	H_{DC} = [-12 kOe : 12 kOe]	d_{CORE} = 50 nm	M_{CORE}
B. *Electromechanical resonance*	b.1 Eigenfrequency study b.2 Frequency-domain perturbation: f = [0:0.01:100] GHz	H_{DC} = 1000 Oe H_{AC} = 15 Oe	d_{CORE} = 25, 50, 100, 150, 200, 250 nm	Resonance frequency f_r
C.1 *Delta-E effect:* Sensor sensitivity	Frequency-domain perturbation: f = [f_r-1 : 0.0001 : f_r+1] GHz	Parametric sweep H_{DC} = [0:1:15] kOe	d_{CORE} = 25, 50, 100, 150, 200, 250 nm	$S = \frac{\Delta f}{\Delta H}; \frac{\Delta E}{E}$ H_{DC} and d_{CORE} so that maximum sensitivity
C.2 *Delta-E effect:* Sensing neural magnetic field through delta-E effect	Frequency-domain perturbation: f = [f_r-1 : 0.0001 : f_r+1] GHz	$H_{EXT} = H_{DC}$ + parametric sweep neural magnetic field [0:5:80] Oe	d_{CORE} = 50 nm	$S = \frac{\Delta f}{\Delta H}$

Fig. 1 Workflow of the computational analysis performed

ME Nanoparticle modeling and characterization

The model of a single MENP was developed and characterized through the finite-element method-based simulation software COMSOL Multiphysics 6.3 (COMSOL n.d.), which enables the coupling of multiple physical domains to model the magnetoelectric effect, following an approach already applied before in in silico studies (Fiocchi et al. 2022; Marrella 2023; Bok et al. 2022). Specifically, the modules involved in the simulations are *Electrostatics*, *Magnetic Field* and *Solid Mechanics*. Also, Multiphysics coupling modules were included, *Piezoelectricity* and *Nonlinear Magnetostriction*, to accurately model the Joule effect, arising from the strain-driven interfacial coupling between the ferromagnetic and ferroelectric domains in ME composites. For a more comprehensive understanding of the mathematical equations underlying the magnetoelectric coupled model refer to the detailed work of Fiocchi and colleagues (Fiocchi et al. 2022).

The nanoparticle is modelled though a 2D-axisymmetric geometry composed by two domains: the magnetostrictive cobalt ferrite core ($CoFe_2O_4$, diameter = 50 nm) and the external piezoelectric shell in barium titanate ($BaTiO_3$, thickness = 15 nm), as shown in Fig. 2. The surrounding environment is defined as a cylindrical domain with a radius of 1000 nm and height of 2000 nm and enclosed by a cylindrical infinite element domain. The material properties of MENPs are listed in Table A1 in the Additional file.

A static magnetic field (H_{DC}) needed to elicit the direct magnetoelectric effect, was simulated by applying a *Magnetic Field* boundary condition to all the boundary faces of the domain.

The MENP was initially characterized by simulating the magnetization of the core in response to an external static magnetic field H_{DC} along z direction and varied linearly in time from −12 kOe to + 12 kOe and vice versa.

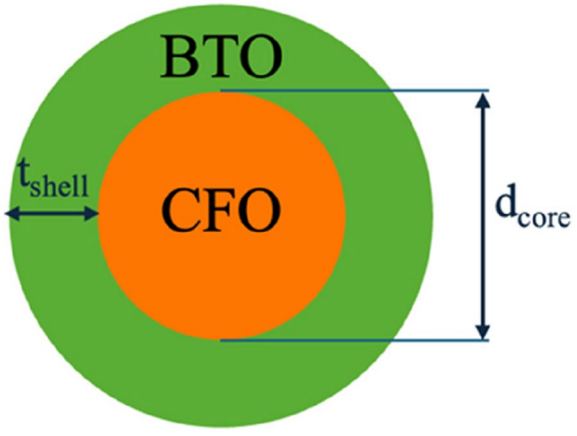

Fig. 2 Geometry of the magnetoelectric nanoparticle: magnetoelectric core in cobalt ferrite and piezoelectric shell in barium titanate

The magnetostrictive CFO core shows a M-H hysteretic loop, that can be described by the Jiles–Atherton (J–A) model (Jiles and Atherton 1986). J-A model parameters, namely interdomain coupling α, pinning loss *k*, magnetization reversibility *c*, domain wall density *a*, were tuned (Khemani et al. 2022; Nikodým et al. 2020) to match the M(H) loop of CFO nanoparticle synthetized by Betal (2016) in terms of coercivity field (H_C), remanent magnetization (M_r) and magnetic saturation (M_s @H_{DC} = 12 kOe).

Since J-A model implements a positive loop, to keep the system stable this relation (1) has to be satisfied (Szewczyk 2019):

$$M_s * \alpha < 3 * a \tag{1}$$

To characterize the MENP at saturation, it was stimulated with a static magnetic field, with a strength sufficient to reach the magnetic saturation of the core, i.e. H_{DC} = 15 kOe. The electric potential of the outer shell, the electric field norm, the strain of the nanoparticle and the magnetization of the core were evaluated and compared with literature values.

The multiphysics characterization was concluded through the definition of the efficiency of the modelled nanoparticle. The magnetoelectric coefficient alpha gives a quantification of the efficiency of the direct ME effect of the nanoparticle and is defined according to Eq. (3):

$$\alpha_{ME} = \frac{\Delta V}{d_{MENP} \bullet H_{DC}} \tag{2}$$

as the ratio between the electric potential difference on the MENP surface [V], and the product of the applied external magnetic field (H_{DC} [Oe]), and the MENP diameter [cm].

A parametric sweep was performed by varying H_{DC} from 0 to 15 kOe in steps of 1 kOe, in order to evaluate the dependence of the MENP efficiency on the applied bias field.

Electromechanical resonance

Previous studies have shown that the stress coupling mechanism in ME composites is highly enhanced when the external magnetic field frequency matches the natural frequency of the sample (Bichurin et al. 2003), leading to improved sensitivity and signal-to-noise ratio (Kiser et al. 2014). To comprehensively characterize the resonant behavior of the modelled ME nanoparticle, two complementary numerical studies were carried out in COMSOL Multiphysics: an *Eigenfrequency study* to determine the intrinsic resonant modes and corresponding eigenfrequencies of the MENP system under a static magnetic bias, and a *Frequency-Domain Perturbation* one to

further analyse the dynamic response of the nanoparticle when subjected to an alternating magnetic field over a broad frequency range. This analysis enabled the characterization of the MENP's resonant peaks in terms of induced electric potential, magnetization, and magnetoelectric coefficient, allowing identification of the dominant resonant mode and assessment of how geometric parameters—specifically the core diameter—influence the overall magnetoelectric performance. The detailed methodology and parameterization of these studies are described below.

The Eigenfrequency study, implemented in COMSOL, was used to compute magnetic, electric or mechanical eigenmodes and eigenfrequencies of the MENP model (Khamkongkaeo et al. 2011; Fiebig 2005). To allow the resolution of the eigenfrequency study the system was linearized around the solution of the MENP subjected to an external static magnetic field of 1000 Oe. This value was chosen as the average of commonly used static magnetic field magnitude in biomedical applications (Pardo and Khizroev 2022) and therefore represents a realistic working point for practical implementation. Linearizing the model around this field strength allows to evaluate the resonance behaviour of the nanoparticle under experimentally relevant conditions, reflecting the most probable operating regime of MENP-based sensing systems. Each eigenmode is characterized by a Q-factor, defined as the ratio between the resonant frequency over the bandwidth; higher Q factor corresponds to a narrower resonance peak in the spectrum (Cai et al. 2020). To simulate a realistic behaviour of the core–shell system the Q-factor, was adjusted in the simulation by introducing mechanical damping. This was implemented by adding *Mechanical damping* and *Damping* subnodes to the shell and core, with isotropic structural loss factor of 0.0001 and 0.00001, respectively. This modelling allowed to overcome the ideal behaviour (i.e. where no damping is included and Q values are in the order of 10^{15}) and obtain eigenmodes characterized by Q values in the order of 10^2–10^4, matching those experimentally found for ME composites (Zaeimbashi et al. 2019; Fiebig 2005; PourhosseiniAsl et al. 2020).

Then, a *Frequency-domain Perturbation* study was performed with the same H_{DC} of 1000 Oe and an alternating magnetic (H_{AC}) field with a peak value of 15 Oe, sweeping the frequency range from 0 to 100 GHz in 0.01 GHz steps. The goal was to identify the resonant peaks of the MENP in terms of electric voltage (V) on the outer shell, the magnetization of the core (M) and the magnetoelectric coefficient alpha (α_{ME}).

From this step the resonant mode is identified as the lowest frequency at which the MENP is characterized by a magnetoelectric coefficient alpha 100 times greater than the off-resonance condition.

The same procedure was repeated for different values of the core diameter (i.e., 25, 50, 100, 150, 200, and 250 nm).

Delta-E effect

The magnetic field sensor investigated in this study is based on the delta-E effect, which is defined as the change in Young's modulus E of the magnetostrictive material arising from the reorientation of the magnetic domains during the magnetization process. The change in E can be evaluated from the resonant frequency shift according to (3) provided by Staruch and colleagues (Staruch et al. 2017):

$$\frac{\Delta E}{E} = \frac{\left(f_{r,sat}^2 - f_{r,min}^2\right)}{f_{r,sat}^2} \tag{3}$$

where $f_{r,sat}$ is the resonance frequency at saturation at very high static magnetic fields (i.e. 30 kOe) and $f_{r,min}$ is the minimum resonance frequency reached by the sensor.

Sensor sensitivity analysis

Once found the resonant mode of interest (from now on "f_r") for each dimension of MENPs investigated, the analysis focused only on frequencies around that value.

MENP used as sensor requires an optimized H_{DC} along with an alternating magnetic field (H_{AC}) characterized by a frequency matching the natural resonant frequency of the MENP (Patil et al. 2021).

A *Frequency-domain Perturbation* study was performed to find the steady-state response of the nanoparticle to an alternating input (H_{AC} peak = 15 Oe) spanning the frequencies around the selected resonant mode from f_r – 1 GHz up to f_r + 1 GHz, with a step size of 0.1 MHz.

To simulate the delta-E effect induced by the static magnetic field used to bias the nanoparticle, it was performed a parametric sweep of H_{DC} from 0 to 15 kOe, with a step of 1 kOe.

For each value of H_{DC} the frequency-domain perturbation was extracted in terms of electric voltage measured on the outer shell. A quantitative analysis was then performed in MATLAB. First, the curve showing the relationship between the resonant frequency and the applied static magnetic field was reconstructed. Next, the maximum sensitivity of the MENP to variations in H_{DC} was computed from the derivative of this curve, and the corresponding value of H_{DC} at which the sensitivity is maximized was identified. The sensitivity of the proposed MENP is defined as (4):

$$S = \frac{\Delta f}{\Delta H} \tag{4}$$

where S is expressed in Hz/nT and represents the resonance frequency shift of the nanoparticle with respect to a change in the applied magnetic field amplitude, mediated by the delta-E effect (Liang et al. 2021; Hui et al. 2015).

To fully characterize the delta- E effect occurring in the nanoparticle, the change in the Young modulus was also computed according to Eq. (3).

The same procedure was followed for different values of the core diameter from 25 to 250 nm.

At the end of this analysis, the values of H_{DC} and the core radius yielding to the maximum sensitivity of the sensor were found.

Sensing neural magnetic field through delta-E effect

Using the core radius leading the highest sensitivity, a *Frequency-domain Perturbation* study was performed with a parametric sweep of the static magnetic field, hereafter referred to as H_{ext}, defined as:

$$H_{ext} = H_{DC}\,[1kOe] + NMF\,[0 - 80Oe] \qquad (5)$$

where H_{ext} takes into account the previously found H_{DC} and the contribution of the neural magnetic field, NMF, to be detected, under the hypothesis that both are aligned in the same direction.

The neural magnetic field generated by the electric activity of brain neurons was varied from 0 to 80 Oe with a step size of 5 Oe in accordance with (Zaeimbashi et al. 2019).

Results

Nanoparticle characterization

Figure 3 shows the hysteretic behaviour of the magnetization (M) of the MENPs core under the application of a static magnetic field (H_{DC}) ranging from −12 kOe up to + 12 kOe. The MENP characterised has a CFO core with the diameter of 50 nm and the BTO shell of 15 nm thickness. The J-A model parameters were tuned to fit the M-H hysteresis loop reported by Betal and colleagues (Betal 2016) and to respect stability Eq. (2).They were found in accordance with literature (Pop and Călţun 2012; 2011; Nikodým et al. 2020): interdomain coupling $\alpha = 1.4$, pinning loss $k = 2*10^5$ A/m, magnetization reversibility $c = 0.4$, domain wall density $a = 1.5*10^5$ A/m.

For conciseness, the full characterization of the MENPs close to saturation including the distribution of the magnetization, of the core to shell strain, and the electric potential on the outer shell, are reported in Fig. A1 in the Additional file and were found consistent with literature values (Fiocchi et al. 2022). Notably, the magnetoelectric coefficient alpha at $H_{DC} = 12$ kOe was found to be 22.9 mV/(cm*Oe) in line with literature (Hossain and Hossain 2022; Rasly et al. 2017).

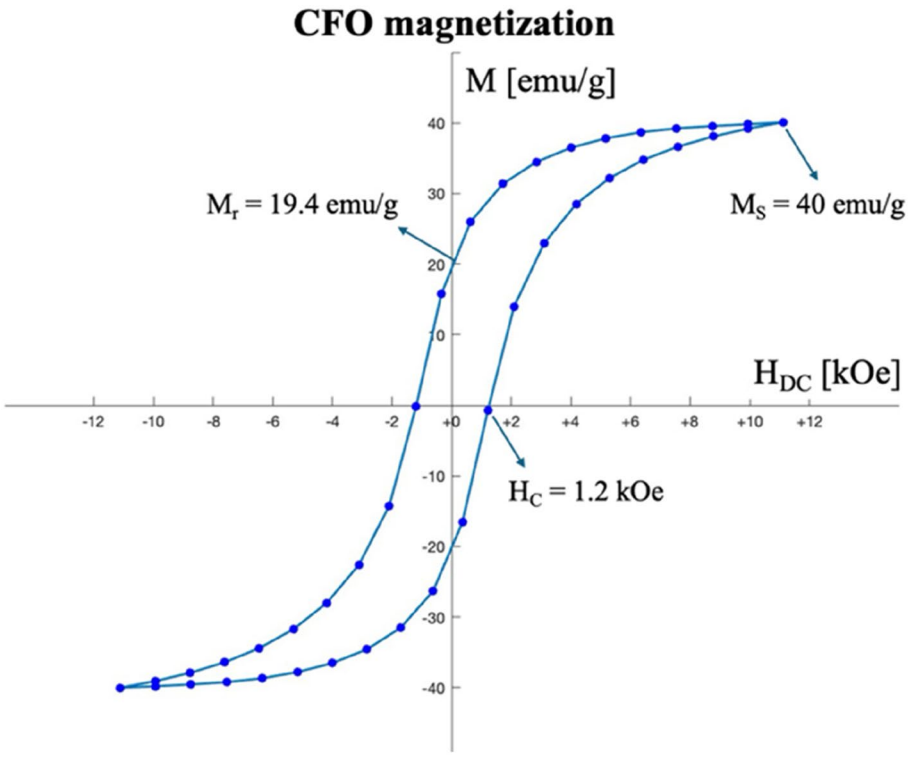

Fig. 3 DC magnetization loops of the CFO core nanoparticle (core diameter = 50 nm)

Electromechanical resonance

As discussed above (see 'Materials and methods' section B. Electromechanical Resonance), the *Eigenfrequency* studies were conducted for core diameters ranging from 25 to 250 nm and shell thickness of 15 nm. From each study six eigenmodes in the GHz range and their correspondent Q-factor were found and reported in the Additional file Table A2.

Figure 4 shows, as an example, the resonant peaks in terms of the magnetoelectric coefficient alpha for the MENP with a core diameter of 50 nm and shell thickness of 15 nm. From that figure, it can be appreciated how despite it would be desirable to operate in the lower range of GHz, the alpha ME magnitude of the actual first resonant mode is less than 1 mV/(cm*Oe), while at the second resonant mode reaches some V/(cm*Oe). The same behaviour has been found for all the core dimensions of nanoparticles. This latter resonance mode will be considered in the following analysis for each nanoparticle.

Figure 5 shows the path followed by the nanoparticles when subjected to an external magnetic field matching the natural resonance frequency of the composite. The applied magnetic field induces magnetostriction in the CFO core, generating mechanical strain transferred to the piezoelectric BTO shell, which in turn produces an electric potential. The corresponding frequency responses show a sharp resonance peak in strain, core magnetization, and electric potential around 36.135 GHz, indicating efficient magnetoelectric conversion at the resonant frequency. Consequently, the resonance happens at both constituent phases of the nanoparticle, from the strain and magnetization of the core to the electric potential of the outer shell.

Figure 6 shows how the resonance frequency of the nanoparticle shifts when the core diameter changes. Increasing the dimension of the nanoparticle the resonance frequency decreases exponentially, while the Q-factor increases, suggesting a more selective bandwidth at f_r for nanoparticles with a larger core. An exponential fit of the data in Fig. 6 shows that increasing the dimension of the core the value of the resonant frequency asymptotically approaches 10 GHz, with a characteristic decay length of 69 nm. This decay represents the scale of the diameter of the core variation causing a drop in resonant frequency of 37% with respect to the initial value above the asymptote.

Sensor sensitivity – delta-E effect

Figures 7 and 8 report the results obtained for the MENP with a core diameter of 50 nm. The plots for the other sized nanoparticles are reported in Fig. A2 in the Additional file. Figure 7 represents the electromechanical resonance frequency of the nanoparticle as a function of the magnetic field used to bias the MENP in the range between 0 and 60 kOe.

From 0 to 2.6 kOe the resonant frequency drops from 36.277 GHz close to 0 Oe reaching a minimum of 35.916 GHz, indicating that the value of Young's modulus E is minimal at this field. This field of 2.6 kOe corresponds to the position where the piezomagnetic coefficient $d_m = d\lambda/dH$ is highest, namely where the magnetic domains in the cobalt ferrite core are easily rotated by the magnetic field.

When the H_{DC} was further increased, the resonance frequency of the sensor increased and saturated at very high magnetic field, 40 kOe, with a maximum resonance frequency of 36.27 GHz. The total maximum resonance frequency shift of the sensor with CFO core = 50 nm was 361 MHz. Under a DC bias field of 1 kOe, the CFO-BTO nanoparticle resonator magnetic field sensor has a sensitivity of 2.59 Hz/nT. For all dimensions of the core investigated, i.e. 25, 50, 100, 150, 200, 250 nm, the maximum

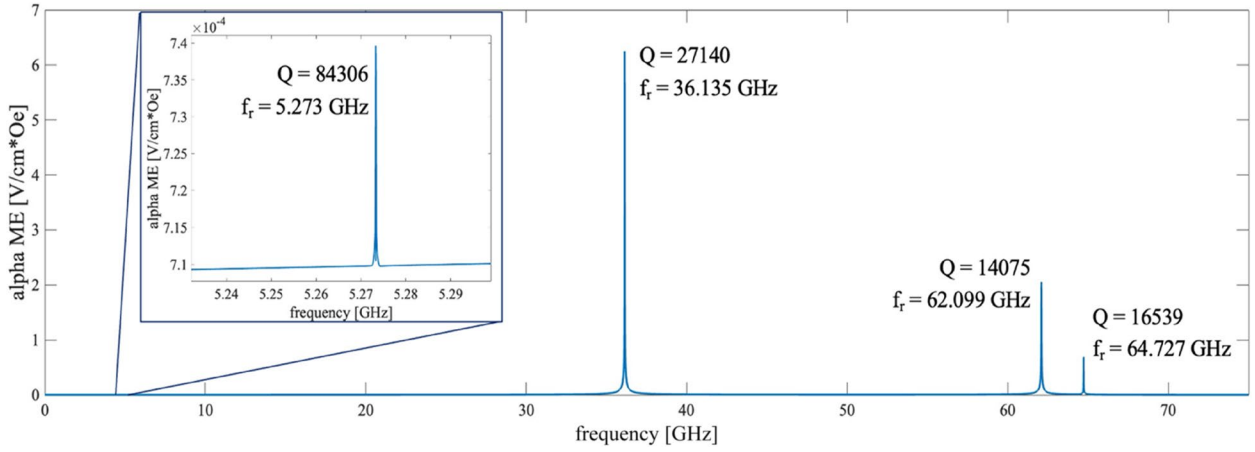

Fig. 4 Resonance peaks with their correspondent Q-factor in the magnetoelectric coefficient alpha when the nanoparticle with core diameter of 50 nm and shell thickness of 15 nm is subjected to a static magnetic field of 1 kOe and an alternating magnetic field of 15 Oe with frequency spanning from 0 to 75 GHz, with a resolution of 10 MHz

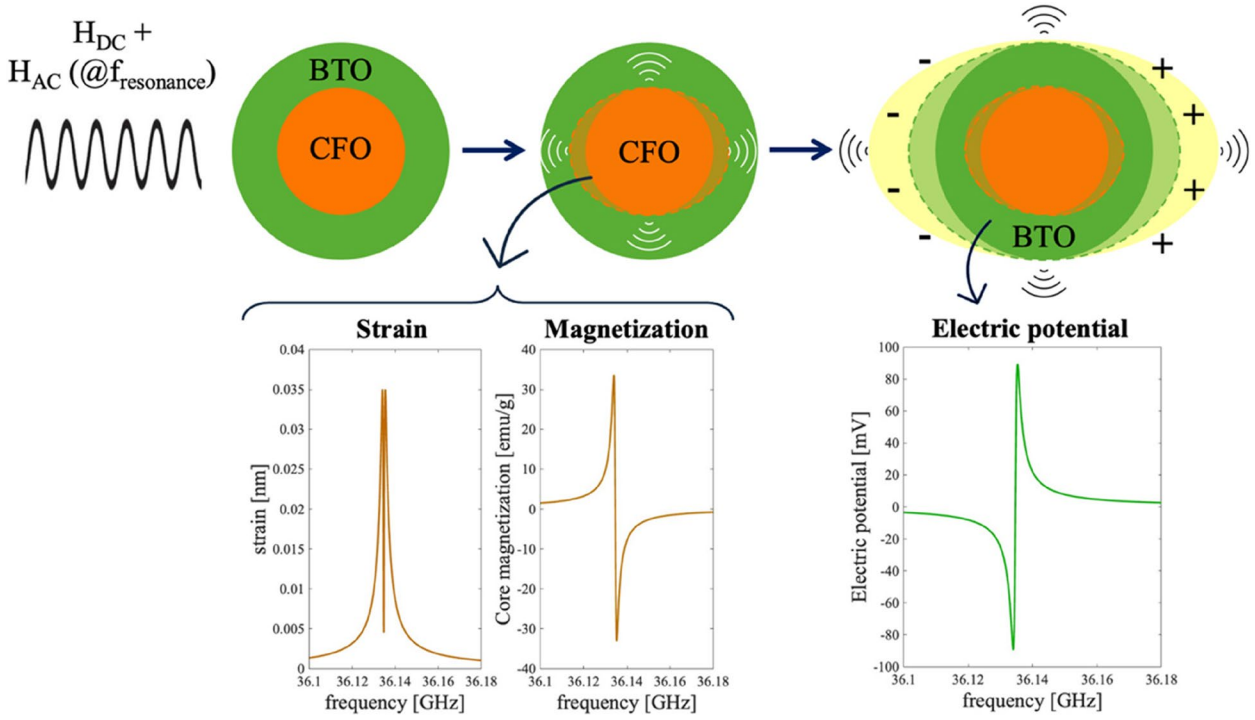

Fig. 5 Visual representation and frequency-dependent responses of a CFO-BTO MENP (core diameter = 50 nm, shell = 15 nm) under combined DC and AC magnetic field excitation at resonance

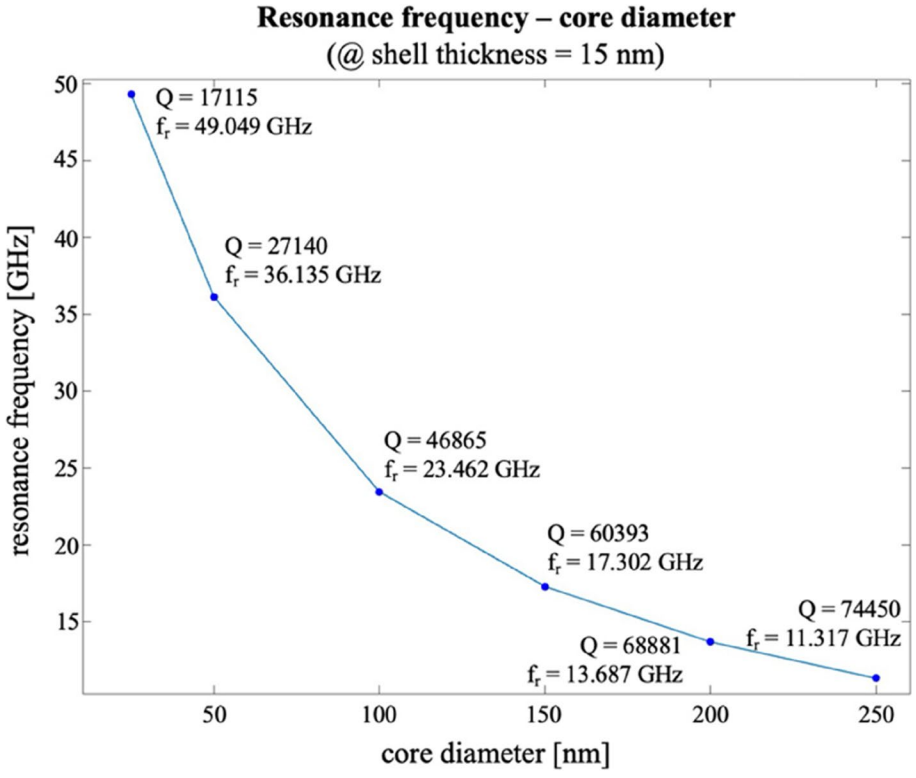

Fig. 6 Effect of core diameter size on the resonance frequency and correspondent Q-factor, when the nanoparticle is subjected to a static magnetic field of 1 kOe and an alternating magnetic field of 15 Oe with frequency spanning from 0 to 75 GHz

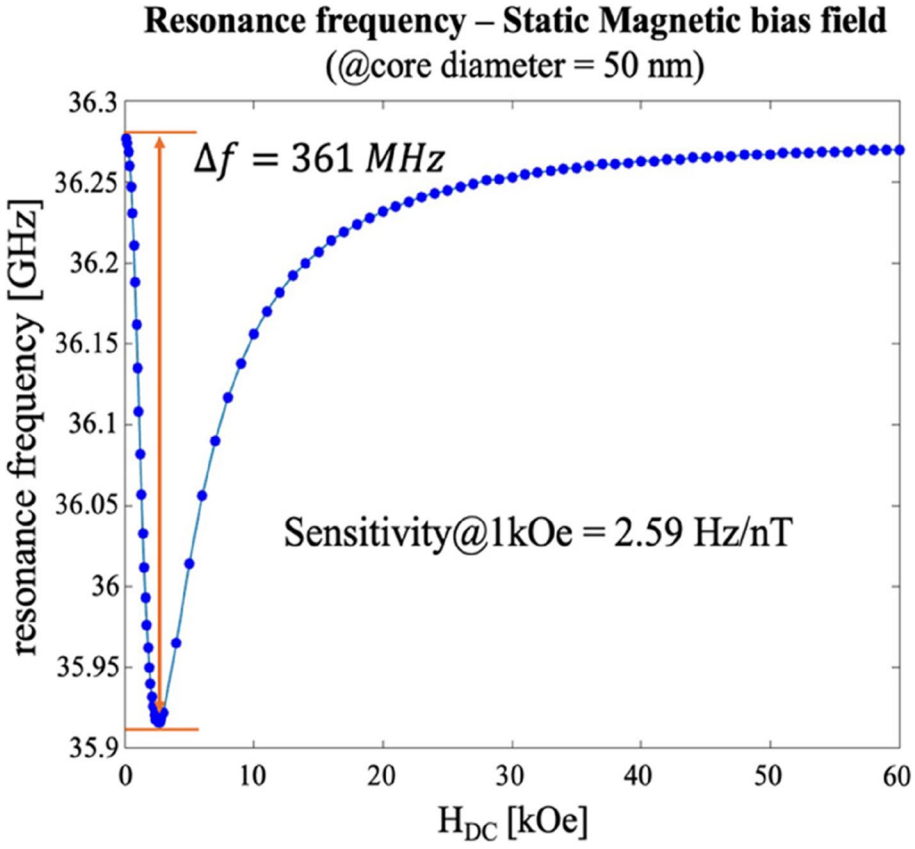

Fig. 7 Electromechanical resonance frequency as a function of static bias magnetic field (H_{DC}) of a MENP with the core of 50 nm. The maximum shift in resonance frequency is of 360 MHz and the maximum sensitivity, df/dH = 2.59 Hz/nT, is reached when H_{DC} = 1kOe

sensitivity is reached at an H_{DC} of 1 kOe and the values found are: 1.81, 2.59, 2.26, 1.79, 1.45, 1.10 Hz/nT, respectively. Among these the nanoparticle with a 50 nm core demonstrated the greatest sensitivity.

The delta-E induced stiffness change was quantified as ΔE/E = 1.94% according to Eq. (3) for MENP with core diameter of 50 nm).

Leveraging on these results, a bias magnetic field of 1 kOe and a core diameter of 50 nm were selected to operate the nanoparticle sensor at an optimal working point for detecting small magnetic field variations. Under these conditions, we further evaluated the sensor's ability to detect magnetic fields generated by neuronal activity.

Figure 8 illustrates the shift in the electromechanical resonance frequency induced by the delta-E effect when the nanoparticle is exposed to neural magnetic fields ranging from 0 to 80 Oe. Notably, a variation of 5 Oe in the external magnetic field results in a measurable resonance frequency shift of approximately 1.4 MHz, demonstrating the high sensitivity of the proposed sensor, in line with other structures of magnetoelectric sensors investigated in literature (Dong et al. 2022).

Discussion

One of the major advantages of measuring the magnetic activity instead of the electrical one from the brain or other organs, is the high spatial and temporal resolution provided by the detection of the magnetic signal, together with a flexible positioning of sensors. Magnetic field travels through tissue without distortion, because the tissues permeability is almost the same as free space (Barnes et al. 2018). Therefore, this characteristic allows also a more precise source-reconstruction of the signals (Gross 2019). This is particularly advantageous in applications such as pre-surgical mapping, where precise localization of neural sources is critical (Fred et al. 2022), or brain-computer interfaces, which benefit from non-invasive high-resolution, real-time monitoring. To date, ME nanoparticles have been mainly investigated for neurostimulation, nano-electroporation and drug delivery, whereas their use as nanoscale sensors of spontaneous neural magnetic activity via the ΔE-effect remains unexplored, representing a novel application for MENP technology and for biomagnetic detection in general.

In this study, we present an in silico theoretical investigation of the potential use of resonant magnetoelectric nanoparticles (MENP) as novel, wireless, non-invasive,

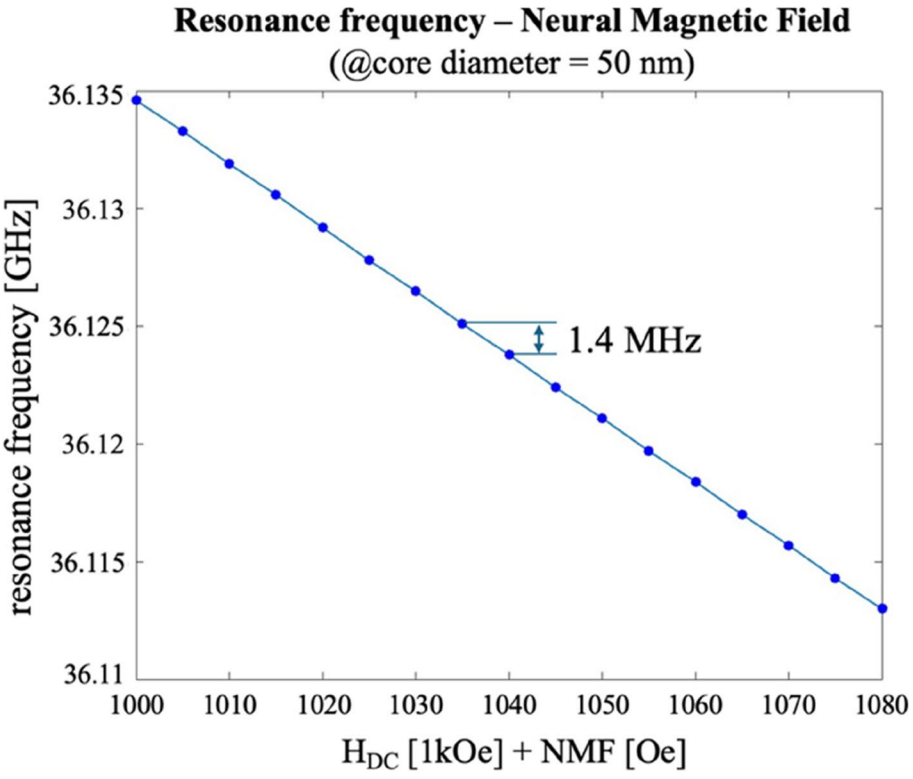

Fig. 8 Electromechanical resonance frequency as a function of a neural magnetic field ranging from 0 to 80 Oe together with a static bias magnetic field H_{DC} = 1kOe, for a MENP with the core of 50 nm

and miniaturized sensitive probes for detecting biomagnetic signals. Specifically, we explored the feasibility of exploiting the delta-E effect in CFO-BTO core–shell MENPs to assess their sensitivity as nanoscale magnetic field sensors. Moreover, as far as we are concerned this is one of the very few studies modeling the resonant behaviour of magnetoelectric nanoparticles.

The single-MENP model provided in this work was tuned to a recently synthetized CFO-BTO nanoparticle (Betal 2016). Specifically, the choice of magnetic parameters and of the Jiles-Atherton model shows a similar behaviour (see Fig. 3) consistent with similar-sized experimental magnetization curves of similarly sized MENPs (Betal 2016; Zhang et al. 2024) and with magnetoelectric coefficient alpha on the order of mV/cm*Oe, in line with those reported in systematic reviews on nanoparticles studies (Song et al. 2022; Hossain and Hossain 2022; Rasly et al. 2017).

The *Eigenfrequency* analysis revealed that the MENP exhibits electromechanical resonance in the GHz range, in accordance with frequencies reported by Popov's work (Popov et al. 2014), which deals with nanoscale ME core–shell composites, and also with Goel's study (Goel et al. 2021) which reported that the resonance frequency of barium hexaferrite nanoparticle is generally above 30 GHz (McNeal et al. 1998).

From Fig. 5 it can be seen how the stress coupling mechanism between the core and the shell leads to a strong increase of the direct magnetoelectric effect. When the frequency of the external exciting field coincides with the frequency of the electromechanical resonance of the nanoparticle, the core experiences a sharp increase in strain (Bichurin et al. 2003), leading to an enhanced magnetoelectric coefficient alpha of two orders of magnitude with respect to the off-resonance condition (Nan et al. 2013).

The electromechanical resonance affects both phases of the multiferroic nanoparticle. The applied magnetic field induces magnetostriction in the CFO core, generating mechanical strain transferred to the piezoelectric BTO shell, which in turn produces an amplified electric potential. Since the chosen amplitude of the alternate magnetic field, i.e. H_{AC} = 15 Oe, is well below the coercivity field of CFO core, i.e. H_C = 1.2 kOe, and the CFO has a non-zero remanent magnetization, the mechanical strain and the H_{AC} have the same frequency. While for H_{AC} greater than H_C, the core undergoes a deformation at twice the frequency of the external excitation (Zhang et al. 2013).

Therefore, the MENP behaves as a ME antenna generating an electromagnetic (EM) wave oscillating at the same frequency of the external exciting field, whose emitted signal could be detected by a receiving antenna tuned at GHz.

The resonance frequency range found for the investigated nanoparticles, as shown in Fig. 4, lies within a regime where EM waves undergo significant absorption in biological tissues. This poses a well-recognized challenge for in vivo applications, as power losses due to tissue attenuation (exceeding 100 dB) limit signal propagation (Zaeimbashi, et al. 2018). Nevertheless, recent advances in electronics have enabled the development of antennas operating in the GHz range, making it feasible to externalize the signal coming from within the body. Examples include the implantable brain computer interface operating in the low GHz range proposed by Simeral and colleagues (Simeral et al. 2021) and the wireless cardiac pacemaker in Feng et al. (2022).

However, our results show that the resonance frequency can be tuned by varying the core diameter, Fig. 6, suggesting that nanoparticle geometry provides a design parameter for application-specific optimization. An increase in core diameter shifts the resonance toward lower frequencies, potentially into the low GHz range, where the dielectric attenuation coefficient of biological tissues is reduces, thereby improving electromagnetic wave penetrations. This trend is consistent with observations reported for thin film ME sensors (Li et al. 2017). Furthermore, some strategies in the synthesis of hexaferrite nanoparticles could be leveraged to further reduce the resonance frequency including cationic substitutions (Trukhanov et al. 2017), sol–gel processing (Surig et al. 1994), solid-state reaction (Yang et al. 2014), co-precipitation method (Tyagi et al. 2011), etc.

In the analysis of resonant sensors, the quality Q-factor represents a critical parameter. In resonance-based sensors, a higher Q factor corresponds to a narrower spectral linewidth, thereby enhancing the ability to detect small perturbations, and directly influences the detection limit of devices such as MENPs (Cai et al. 2020). As shown in Fig. 6, an increase in core diameter yields a higher Q-factor, indicating improved selectivity of the nanoparticle response.

The resonant sensor here investigated relies on the delta-E effect, based on the dependency of the Young's modulus on the external magnetic field. In this process, the magnetostrictive core rearranges the magnetic domains according to the external magnetic field, changing the mechanical properties of the core, and, as a consequence, a shift in the electromechanical resonance frequency according to Eq. (3).

The non-linear behaviour of the delta-E effect observed in the simulations, Fig. 7, can be attributed to the magnetostrictive susceptibility χ, a major determinant of the delta-E effect (Ludwig and Quandt 2002). In non-linear magnetostrictive material such as cobalt ferrite, the magnetization follows a hysteretic behaviour, causing a non-linear and history dependent χ (Kumar and Arockiarajan 2022). Behaviour of the resonant frequency of MENPs follows the same of magnetoelectric thin-film and cantilevers millimetric structures, as reported in Zaeimbashi et al. (2019) (Nan et al. 2013; Staruch et al. 2017; Kagomiya et al. 2012); however, resonant phenomena at the nanoparticle scale are still under investigated.

According to our findings, the maximum sensitivity for the MENP to detect an external magnetic field change is obtained with an external bias of static magnetic field of 1 kOe. Such a bias field is a fundamental for ME sensors (Patil et al. 2021), and when combined with high-frequency alternating H_{AC} excitation, serves to enhance the overall ME effect.

To the best of our knowledge, this is the first study to systematically investigate the influence of varying the static magnetic bias on sensor sensitivity, thereby identifying the optimal working point. Previous studies have primarily focused on selecting the bias field that maximizes the magnetoelectric coefficient alpha, without evaluating its impact on the actual sensing performance (Hayes et al. 2019).

For what concern the sensitivity, the results show an increase up to a maximum at a core diameter of 50 nm, followed by a subsequent decrease. This nonlinear behaviour of the sensitivity on core dimension can be plausibly attributed to the intrinsic non-linearity of the direct magnetoelectric coupling. From previous studies it has been shown how the magnetoelectric coefficient alpha nonlinearly depends on the core dimensions (Fiocchi et al. 2022).

The sensor investigated here works at high frequencies for which is known that delta-E effect is known to be attenuated due to the stiffening of the Young's modulus (Spetzler et al. 2019). Consequently, the resonance frequency shift typically occurs under magnetic field strengths in the kOe range. Nevertheless, as shown in Fig. 8, the sensitivity found for the investigated nanoparticle is still comparable to that reported for larger thin-film structures (Li et al. 2017) and a change in the static magnetic field of 1 nT causes a shift in resonance of ~ 2 Hz. This value is in line with the order of magnitude of the neural magnetic field in proximity of the axon, as reported in Matlachov et al. (2004) (Caruso et al. 2017).

This highlights the importance of developing highly selective resonant antennas with narrow detection bandwidth cantered on the natural resonance frequency of the nanoparticle (Zaeimbashi, et al. 2018), thereby enabling the resolution of frequency shifts on the order of a few Hz.

Although the present study provides promising indications about the feasibility of MENPs as nanoscale, minimally invasive and wireless probes of biomagnetic signals, several limitations should be acknowledged.

First, the present computational study is focused on the deterministic sensitivity analysis, expressed in Hz/nT, and no noise modelling was included in the simulations. Full noise model will be included in future studies in order to define the limit of detection of the modelled MENP. Moreover, this study relies on the use of only one MENP, while a more realistic scenario would involve a cluster. In such condition, it will be necessary to study the MENP-to-MENP interaction. From a synthesis perspective, variability across MENPs in size and morphology, could introduce differences in their resonant frequencies and magnetoelectric response, potentially impacting sensing capability. These aspects will be systematically addressed in future research to bridge the gap between computational modelling and experimental implementation.

Conclusion

In summary, this in-silico study demonstrates the feasibility of using resonant magnetoelectric nanoparticles to detect the magnetic fields generated by the electrical activity of biological tissues, by exploiting the delta-E effect. Our findings reveal that MENPs, specifically core–shell structures composed of cobalt ferrite and barium titanate, can act as wireless, self-powered magnetic sensors. When excited by an external magnetic field at their electromechanical resonance frequency, these nanoparticles exhibit a pronounced magnetoelectric response and emit electromagnetic radiation, thereby obviating the need for embedded power sources such as batteries.

The simulations further show that MENPs display high sensitivity to external magnetic field variations, with sensitivity depending non-linearly on core diameter. This relationship opens the possibility to tailor their resonance frequency by adjusting nanoparticle geometry, grain size, or by adopting more anisotropic shapes, thus tuning the sensor's operating range for specific biomedical applications. This design flexibility makes MENPs a promising alternative to conventional technologies such as SQUIDs or invasive magnetic sensors.

Altogether, these theoretical insights pave the way for the development of next-generation wireless nanoscale magnetic sensors, with prospective applications in neural interfacing, minimally invasive diagnostics, and magnetically responsive smart materials.

Supplementary Information

The online version contains supplementary material available at https://doi.org/10.1186/s42234-025-00198-1.

Supplementary Material 1.

Authors' contributions

G.C., E.C., S.F. and P.R. conceived and designed the study; G.C., E.C. and S.F. investigated and analyzed the data; G.C. wrote the manuscript text and E.C., S.F., and P.R., dedicated to the review and editing. All authors have read and agreed to the published version of the manuscript.

Funding

This work was supported by the Italian Ministry of Research through the Complementary Actions of the National Recovery and Resilience Plan (NRRP) "Fit4MedRob—Fit for Medical Robotics" under Grant PNC0000007.

Declarations

Ethics approval and consent to participate

Not applicable.

Competing interests

The authors declare that the research was conducted in the absence of any commercial or financial relationships that could be construed as a potential conflict of interest.

Received: 24 October 2025 / Accepted: 14 December 2025
Published online: 09 January 2026

References

Abdelazim H. Magneto-electric nanocarriers for drug delivery: an overview. J Drug Deliv Sci Technol. 2017;37:46–50. https://doi.org/10.1016/j.jddst.2016.11.003.
Barnes GR, Hillebrand A, Fawcett IP, Singh KD. Realistic spatial sampling for MEG beamformer images. Hum Brain Mapp. 2004;23(2):120–7. https://doi.org/10.1002/hbm.20047.
Barnes FS, Greenebaum B. Biological and medical aspects of electromagnetic fields. CRC Press. 2018. https://doi.org/10.1201/9781315221557.
Betal S, et al. Magneto-elasto-electroporation (MEEP): in-vitro visualization and numerical characteristics. Sci Rep. 2016. https://doi.org/10.1038/srep32019.
Bichurin I, Filippov A, Petrov M, Laletsin M, Paddubnaya N, Srinivasan G. Resonance magnetoelectric effects in layered magnetostrictive-piezoelectric composites. Phys Rev B. 2003. https://doi.org/10.1103/PhysRevB.68.132408.
Bok I, Haber I, Qu X, Hai A. In silico assessment of electrophysiological neuronal recordings mediated by magnetoelectric nanoparticles. Sci Rep. 2022. https://doi.org/10.1038/s41598-022-12303-4.
Cai L, Pan J, Hu S. Overview of the coupling methods used in whispering gallery mode resonator systems for sensing. Opt Lasers Eng. 2020. https://doi.org/10.1016/j.optlaseng.2019.105968.
Caruso L, et al. In vivo magnetic recording of neuronal activity. Neuron. 2017;95(6):1283-1291.e4. https://doi.org/10.1016/j.neuron.2017.08.012.
Cohen D. Magnetoencephalography: detection of the brain's electrical activity with a superconducting magnetometer. Science. 1972;175(4022):664–6. https://doi.org/10.1126/science.175.4022.664.
Cohen D, Edelsack EA, Zimmerman JE. Magnetocardiograms taken inside a shielded room with a superconducting point-contact magnetometer. Appl Phys Lett. 1970;16(7):278–80. https://doi.org/10.1063/1.1653195.
COMSOL AB. COMSOL Multiphysics®. Stockholm, Sweden. n.d. Available from: www.comsol.com.
Corral-Flores V, Bueno-Baqués D, Ziolo RF. Synthesis and characterization of novel CoFe2O4–BaTiO3 multiferroic core–shell-type nanostructures. Acta Mater. 2010;58(3):764–9. https://doi.org/10.1016/j.actamat.2009.09.054.
Dong C, et al. Thin film magnetoelectric sensors toward biomagnetism: materials, devices, and applications. Adv Electron Mater. 2022. https://doi.org/10.1002/aelm.202200013.
Eerenstein W, Mathur ND, Scott JF. Multiferroic and magnetoelectric materials. Nature. 2006. https://doi.org/10.1038/nature05023.
Ekreem NB, Olabi AG, Prescott T, Rafferty A, Hashmi MSJ. An overview of magnetostriction, its use and methods to measure these properties. J Mater Process Technol. 2007;191(1–3):96–101. https://doi.org/10.1016/j.jmatprotec.2007.03.064.
Elzenheimer E, et al. Investigation of converse magnetoelectric thin-film sensors for magnetocardiography. IEEE Sens J. 2023;23(6):5660–9. https://doi.org/10.1109/JSEN.2023.3237910.
Feng Y, Li Z, Qi L, Shen W, Li G. A compact and miniaturized implantable antenna for ISM band in wireless cardiac pacemaker system. Sci Rep. 2022. https://doi.org/10.1038/s41598-021-04404-3.

Fiebig M. Revival of the magnetoelectric effect. J Phys D Appl Phys. 2005. https://doi.org/10.1088/0022-3727/38/8/R01.
Fiocchi S, et al. Modeling of core-shell magneto-electric nanoparticles for biomedical applications: effect of composition, dimension, and magnetic field features on magnetoelectric response. PLoS One. 2022. https://doi.org/10.1371/journal.pone.0274676.
Fred AL, et al. A brief introduction to magnetoencephalography (MEG) and its clinical applications. Brain Sci. 2022. https://doi.org/10.3390/brainsci12060788.
Galletta V, Bonato M, Fiocchi S, Chiaramello E. Wireless peripheral nerve recording by magnetoelectric nanoparticles. IEEE Sens J. 2025. https://doi.org/10.1109/JSEN.2025.3542983.
Goel S, et al. Microwave absorption study of composites based on CQD@BaTiO3 core shell and BaFe12O19 nanoparticles. J Alloys Compd. 2021. https://doi.org/10.1016/j.jallcom.2020.157411.
Gojdka B, et al. Fully integrable magnetic field sensor based on delta-E effect. Appl Phys Lett. 2011;99(22):223502. https://doi.org/10.1063/1.3664135.
Gross J. Magnetoencephalography in cognitive neuroscience: a primer. Neuron. 2019;104(2):189–204. https://doi.org/10.1016/j.neuron.2019.07.001.
Hadjikhani A, et al. Biodistribution and clearance of magnetoelectric nanoparticles for nanomedical applications using energy dispersive spectroscopy. Nanomedicine. 2017;12(15):1801–22. https://doi.org/10.2217/nnm-2017-0080.
Hayes P, et al. Converse magnetoelectric composite resonator for sensing small magnetic fields. Sci Rep. 2019. https://doi.org/10.1038/s41598-019-52657-w.
Hossain S, Hossain S. Magnetic and optical characterization of cobalt ferrite-barium titanate core-shell for biomedical applications. IEEE Trans Magn. 2022. https://doi.org/10.1109/TMAG.2021.3140037.
Hui Y, Nan T, Sun NX, Rinaldi M. High resolution magnetometer based on a high frequency magnetoelectric MEMS-CMOS oscillator. J Microelectromech Syst. 2015;24(1):134–43. https://doi.org/10.1109/JMEMS.2014.2322012.
Jiles DC, Atherton DL. Theory of ferromagnetic hysteresis. J Magn Magn Mater. 1986;61(1–2):48–60. https://doi.org/10.1016/0304-8853(86)90066-1.
Kagomiya I, Hayashi Y, Kakimoto KI, Kobayashi K. Magnetic field dependence of piezoelectric resonance frequency in CoFe 2O 4-BaTiO 3 composites. J Magn Magn Mater. 2012;324(15):2368–72. https://doi.org/10.1016/j.jmmm.2012.03.002.
Khamkongkaeo A, Jantaratana P, Sirisathitkul C, Yamwong T, Maensiri S. Frequency-dependent magnetoelectricity of CoFe 2O 4-BaTiO 3 particulate composites. Trans Nonferrous Met Soc China. 2011;21(11):2438–42. https://doi.org/10.1016/S1003-6326(11)61033-9.
Khemani V, Azarian MH, Pecht MG. Efficient identification of Jiles-Atherton model parameters using space-filling designs and genetic algorithms. Eng. 2022;3(3):364–72. https://doi.org/10.3390/eng3030026.
Kiser J, et al. Magnetostrictive stress reconfigurable thin film resonators for near direct current magnetoelectric sensors. Appl Phys Lett. 2014. https://doi.org/10.1063/1.4866044.
Körber R, et al. SQUIDs in biomagnetism: a roadmap towards improved healthcare. Supercond Sci Technol. 2016;29(11):113001. https://doi.org/10.1088/0953-2048/29/11/113001.
Kozielski KL, et al. A P P L I E D S C I E N C E S A N D E N G I N E E R I N G Nonresonant powering of injectable nanoelectrodes enables wireless deep brain stimulation in freely moving mice. 2021. Available: https://www.science.org
Kujawska M, Kaushik A. Exploring magneto-electric nanoparticles (MENPs): a platform for implanted deep brain stimulation. Neural Regen Res. 2023;18(1):129. https://doi.org/10.4103/1673-5374.340411.
Kumar A, Arockiarajan A. Evolution of nonlinear magneto-elastic constitutive laws in ferromagnetic materials: a comprehensive review. J Magn Magn Mater. 2022. https://doi.org/10.1016/j.jmmm.2021.168821.
Kwon H, et al. Non-invasive magnetocardiography for the early diagnosis of coronary artery disease in patients presenting with acute chest pain. Circ J. 2010;74(7):1424–30. https://doi.org/10.1253/circj.CJ-09-0975.
Li M, et al. Ultra-sensitive NEMS magnetoelectric sensor for picotesla DC magnetic field detection. Appl Phys Lett. 2017. https://doi.org/10.1063/1.4979694.
Li J, Shen Y, Shen C, Ning X, Xiang M. Advances of magnetocardiography in application of adult and fetal cardiac diseases. Front Cardiovasc Med. 2025. https://doi.org/10.3389/fcvm.2025.1522467.
Liang X, et al. Roadmap on magnetoelectric materials and devices. IEEE Trans Magn. 2021. https://doi.org/10.1109/TMAG.2021.3086635.
Lombardi G, Sorbo AR, Guida G, La Brocca L, Fenici R, Brisinda D. Magnetocardiographic classification and non-invasive electro-anatomical imaging of outflow tract ventricular arrhythmias in recreational sport activity practitioners. J Electrocardiol. 2018;51(3):433–9. https://doi.org/10.1016/j.jelectrocard.2018.02.004.
Ludwig A, Quandt E. Optimization of the ΔE effect in thin films and multilayers by magnetic field annealing. IEEE Trans Magn. 2002;38(5):2829–31. https://doi.org/10.1109/TMAG.2002.802467.
Marrella A, et al. Magnetoelectric nanoparticles shape modulates their electrical output. Front Bioeng Biotechnol. 2023. https://doi.org/10.3389/fbioe.2023.1219777.
Martins P, Brito-Pereira R, Ribeiro S, Lanceros-Mendez S, Ribeiro C. Magnetoelectrics for biomedical applications: 130 years later, bridging materials, energy, and lifeWriting. 2024. Elsevier Ltd. https://doi.org/10.1016/j.nanoen.2024.109569.
Matlachov AN, Volegov PL, Espy MA, George JS, Kraus RH. SQUID detected NMR in microtesla magnetic fields. J Magn Reson. 2004;170(1):1–7. https://doi.org/10.1016/j.jmr.2004.05.015.
McNeal MP, Jang SJ, Newnham RE. The effect of grain and particle size on the microwave properties of barium titanate (BaTiO3). J Appl Phys. 1998;83(6):3288–97. https://doi.org/10.1063/1.367097.
Murzin D, et al. Ultrasensitive magnetic field sensors for biomedical applications. MDPI AG. 2020. https://doi.org/10.3390/s20061569.
Nakamura A, et al. Electromagnetic signatures of the preclinical and prodromal stages of Alzheimer's disease. Brain. 2018;141(5):1470–85. https://doi.org/10.1093/brain/awy044.
Nan T, Hui Y, Rinaldi M, Sun NX. Self-biased 215MHz magnetoelectric NEMS resonator for ultra-sensitive DC magnetic field detection. Sci Rep. 2013. https://doi.org/10.1038/srep01985.
Nguyen T, et al. In vivo wireless brain stimulation via non-invasive and targeted delivery of magnetoelectric nanoparticles. Neurotherapeutics. 2021;18(3):2091–106. https://doi.org/10.1007/s13311-021-01071-0.
Nikodým M, Luňáček J, Jirásková Y, Janoš P, Juřjca J, Životský O. Fe-oxide/CeO2composites - Magnetization curves and their analyses using the Jiles-Atherton model. in Acta Physica Polonica A, Polish Academy of Sciences. 2020:601–603. https://doi.org/10.12693/APhysPolA.137.601.
Pardo M, Khizroev S. Where do we stand now regarding treatment of psychiatric and neurodegenerative disorders? Considerations in using magnetoelectric nanoparticles as an innovative approach. Wires Nanomed Nanobiotechnol. 2022. https://doi.org/10.1002/wnan.1781.
Park J, Hill PM, Chung N, Hugenholtz PG, Jung F. Magnetocardiography predicts coronary artery disease in patients with acute chest pain. Ann Noninvasive Electrocardiol. 2005;10(3):312–23. https://doi.org/10.1111/j.1542-474X.2005.00634.x.
Parker KK, Wikswo JP. A model of the magnetic fields created by single motor unit compound action potentials in skeletal muscle. IEEE Trans Biomed Eng. 1997. https://doi.org/10.1109/10.634647.
Patil DR, Kumar A, Ryu J. Recent progress in devices based on magnetoelectric composite thin films. Sensors (Basel). 2021. https://doi.org/10.3390/s21238012.
Pethig R. Dielectric properties of body tissues. Clin Phys Physiol Meas. 1987;8(4A):5–12. https://doi.org/10.1088/0143-0815/8/4A/002.
Pop NC, Caltun OF. Jiles-atherton model used in the magnetization process study for the composite magnetoelectric materials based on cobalt ferrite and barium titanate. Can J Phys. 2011;89(7):787–92. https://doi.org/10.1139/p11-057.
Pop NC, Căltun OF. Using the jiles atherton model to analyze the magnetic properties of magnetoelectric materials: (BaTiO 3) x (CoFe 2 O 4) 1–x. Indian J Phys. 2012;86(4):283–9. https://doi.org/10.1007/s12648-012-0055-9.
Popov M, Sreenivasulu G, Petrov VM, Chavez FA, Srinivasan G. High frequency magneto-dielectric effects in self-assembled ferrite-ferroelectric core-shell nanoparticles. AIP Adv. 2014. https://doi.org/10.1063/1.4895591.
PourhosseiniAsl MJ, et al. Versatile power and energy conversion of magnetoelectric composite materials with high efficiency via electromechanical resonance. Nano Energy. 2020;70. https://doi.org/10.1016/j.nanoen.2020.104506.
Rasly M, Afifi M, Shalan AE, Rashad MM. A quantitative model based on an experimental study for the magnetoelectric coupling at the interface of cobalt ferrite–barium titanate nanocomposites. Appl Phys A Mater Sci Process. 2017. https://doi.org/10.1007/s00339-017-0954-x.
Reermann J, et al. Evaluation of magnetoelectric sensor systems for cardiological applications. Measurement. 2018;116:230–8. https://doi.org/10.1016/j.measurement.2017.09.047.
Roth BJ. Biomagnetism: the first sixty years. Sensors. 2023. https://doi.org/10.3390/s23094218.

Simeral JD, et al. Home use of a percutaneous wireless intracortical brain-computer interface by individuals with tetraplegia. IEEE Trans Biomed Eng. 2021;68(7):2313–25. https://doi.org/10.1109/TBME.2021.3069119.
Song H, Listyawan MA, Ryu J, MDPI. Core–shell magnetoelectric nanoparticles: materials, synthesis, magnetoelectricity, and applications. Actuators. 2022. https://doi.org/10.3390/act11120380.
Soufineyestani M, Dowling D, Khan A. Electroencephalography (EEG) technology applications and available devices. Appl Sci. 2020. https://doi.org/10.3390/app10217453.
Spetzler B, Golubeva EV, Müller C, McCord J, Faupel F. Frequency dependency of the delta-E effect and the sensitivity of delta-E effect magnetic field sensors. Sensors (Basel). 2019. https://doi.org/10.3390/s19214769.
Srinivasan G, Rasmussen ET, Gallegos J, Srinivasan R, Bokhan YI, Laletin VM. Magnetoelectric bilayer and multilayer structures of magnetostrictive and piezoelectric oxides. Phys Rev B. 2001. https://doi.org/10.1103/PhysRevB.64.214408.
Staruch M, Yang MT, Li JF, Dolabdjian C, Viehland D, Finkel P. Frequency reconfigurable phase modulated magnetoelectric sensors using Δe effect. Appl Phys Lett. 2017. https://doi.org/10.1063/1.4994663.
Sternickel K, Braginski AI. Biomagnetism using SQUIDs: status and perspectives. Supercond Sci Technol. 2006;19(3):S160–71. https://doi.org/10.1088/0953-2048/19/3/024.
Surig C, Hempel KA, Bonnenberg D. Hexaferrite particles prepared by sol-gel technique. IEEE Trans Magn. 1994;30(6):4092–4. https://doi.org/10.1109/20.333999.
Szewczyk R. Progress in development of Jiles-Atherton model of magnetic hysteresis. in AIP Conference Proceedings, American Institute of Physics Inc. 2019. https://doi.org/10.1063/1.5119498.
Tolstrup K, et al. Non-invasive resting magnetocardiographic imaging for the rapid detection of ischemia in subjects presenting with chest pain. Cardiology. 2006;106(4):270–6. https://doi.org/10.1159/000093490.
Trukhanov SV, et al. Investigation into the structural features and microwave absorption of doped barium hexaferrites. Dalton Trans. 2017;46(28):9010–21. https://doi.org/10.1039/C7DT01708A.
Tyagi S, Baskey HB, Agarwala RC, Agarwala V, Shami TC. Development of hard/soft ferrite nanocomposite for enhanced microwave absorption. Ceram Int. 2011;37(7):2631–41. https://doi.org/10.1016/j.ceramint.2011.04.012.
Vezzoni A, Chiaramello E, Galletta V, Bonato M, Parazzini M, Fiocchi S. Computational insights into magnetoelectric nanoparticles for neural stimulation. Front Neurosci. 2025;19:1583152. https://doi.org/10.3389/fnins.2025.1583152.
Yang Y, Liu X, Jin D, Ma Y. Structural and magnetic properties of La–Co substituted Sr–Ca hexaferrites synthesized by the solid state reaction method. Mater Res Bull. 2014;59:37–41. https://doi.org/10.1016/j.materresbull.2014.06.003.
Zaeimbashi M, et al. NanoNeuroRFID: a wireless implantable device based on magnetoelectric antennas. IEEE J Electromagn RF Microw Med Biol. 2019;3(3):206–15. https://doi.org/10.1109/JERM.2019.2903930.
Zaeimbashi M, et al. NanoNeuroRFID: A Low Loss Brain Implantable Device Based on Magnetoelectric Antenna, in 2018 IEEE International Microwave Biomedical Conference (IMBioC), IEEE. 2018:205–207. https://doi.org/10.1109/IMBIOC.2018.8428892.
Zhang K, Zhang L, Fu L, Li S, Chen H, Cheng ZY. Magnetostrictive resonators as sensors and actuators. Sens Actuators A-Phys. 2013;200:2–10. https://doi.org/10.1016/j.sna.2012.12.013.
Zhang E, et al. Ab initio physics considerations in the design of wireless and non-invasive neural recording systems using magnetoelectric nanoparticles. IEEE Trans Magn. 2023;59(10). https://doi.org/10.1109/TMAG.2023.3300791.
Zhang E, et al. Controlling action potentials with magnetoelectric nanoparticles. Brain Stimul. 2024;17(5):1005–17. https://doi.org/10.1016/j.brs.2024.08.008.
Zuo S, et al. Ultrasensitive magnetoelectric sensing system for pico-tesla magnetomyography. IEEE Trans Biomed Circuits Syst. 2020;14(5):971–84. https://doi.org/10.1109/TBCAS.2020.2998290.

Publisher's Note